CrossMark

The Fundamental Plane of GRBs

Xu Zhang[1] and Quan-Gui Gao[1,2]
[1] Department of Physics, Yuxi Normal University, Yuxi 653100, China; qggao@yxnu.edu.cn
[2] Key Laboratory of Astroparticle Physics of Yunnan Province, Kunming 650091, China

Abstract

Gamma-ray bursts (GRBs) exhibit powerful radiation and relativistic jets similar to blazars. However, the central engine of GRBs remains unknown. In this paper, we use the fundamental plane to analyze a sample of GRBs with measured mass. We extend, over ~12 orders of magnitude, the correlation analysis and fundamental plane with a sample of X-ray binaries, active galactic nuclei (AGNs) including blazars, and brightest cluster galaxies. The fundamental plane of our de-beamed sample, with a measured mass ($\log L_R = (0.60 \pm 0.03)\log L_X + (0.78 \pm 0.02)\log M + 7.23 \pm 0.95$), closely aligns with the findings of previous work on AGNs. This finding suggests that GRBs adhere to the fundamental plane of AGNs and supports the theory proposed in previous work that the central engine of GRBs may be black holes. This observation provides a plausible explanation for the striking similarities between GRBs and AGNs.

Key words: (stars:) gamma-ray burst: general – radiation mechanisms: general – galaxies: active

1. Introduction

The investigation of similarities among stellar, intermediate and supermassive black holes (BHs) represents a long-standing and interesting question (White et al. 1984; Mirabel & Rodriguez 1999; Meier 2003; Wang & Dai 2017). Previous works have suggested that different types of BH sources may exhibit similar characteristics, including the accretion process (McHardy et al. 2006), radiation mechanism (Wang et al. 2014), energetics of relativistic jets (Nemmen et al. 2012) and statistical properties of X-ray flares (Wang et al. 2015). Merloni et al. (2003) and Falcke et al. (2004) found a strong correlation between radio luminosity and X-ray luminosity in active galactic nuclei (AGNs), which they referred to as the fundamental plane, after taking into account BH mass. This correlation closely resembles the correlation observed in the X-ray binaries (XRBs) GX339-4 and V404 Cyg, first discovered by Corbel et al. (2000) and Gallo et al. (2003). Subsequent studies have provided further confirmation of the existence of the fundamental plane (Körding et al. 2006; Li et al. 2008; Yuan et al. 2009; Gültekin et al. 2014). Nevertheless, some research has cast doubt on the reliability of the fundamental plane. Merloni et al. (2006) suggest that intrinsic characteristics of BHs should be considered due to distance artifacts, and Körding et al. (2006) found that some XRBs may not adhere to the fundamental plane. Later studies identified additional outliers (Jonker et al. 2010; Coriat et al. 2011; Ratti et al. 2012). Moreover, when examining the low/hard state of XRBs and low-luminosity AGNs, Körding et al. (2006) found that the fundamental plane is much tighter than in the full sample, indicating that radiatively inefficient BH

sources are the most appropriate for the fundamental plane. Dong et al. (2014) and Xie & Yuan (2017) also established the fundamental plane for radiatively efficient BHs. However, the fundamental plane has also been found to accurately fit brightest cluster galaxies (BCGs) (Mezcua et al. 2018) and O_{III} luminosity of AGNs (Heckman et al. 2005).

Gamma-ray bursts (GRBs) are the most powerful electromagnetic explosions in the universe (Wang & Dai 2017). The central engine responsible for these bursts is still unknown, but two main theories suggest that massive stars (Woosley 1993) or mergers of compact stars (Eichler et al. 1989; Nakar 2007) could be their progenitors. Interestingly, GRBs share some similar properties with AGNs, such as their variability (Wu et al. 2016; Xiong et al. 2017, 2020) and radiation mechanisms (Lyu et al. 2014). Both GRBs and blazars also exhibit powerful relativistic jets, with X-ray and radio emissions likely originating from these jets (Piran 2004; Zhang & Mészáros 2004; Gehrels et al. 2009; Xiong & Zhang 2014; Kumar & Zhang 2015; Mezcua et al. 2018). Several studies have suggested that blazars and GRBs have similar radiation mechanisms (Wang et al. 2014, 2015; Zhang et al. 2017). These findings suggest that GRBs could be a type of BH source and that they may follow the fundamental plane of AGNs and XRBs (Wang & Dai 2017; Zhu et al. 2019; Constantinos et al. 2022).

Therefore, it is essential to investigate whether blazars and GRBs follow the fundamental plane of AGNs and XRBs. Lü et al. (2015) and Wang & Dai (2017) extended the fundamental plane to GRBs and found a correlation between X-ray luminosity and radio luminosity for XRBs, AGNs and GRBs.

However, the results of Lü et al. (2015) slightly differ from the works of Corbel et al. (2000) and Gallo et al. (2003). The fundamental plane derived by Wang & Dai (2017), which included estimated mass values for GRBs ($3M_\odot$ and $10M_\odot$), suggests that the influence of the beaming factor on the fundamental plane is weak but did not include the sample of blazars.

In this paper, we aim to extend the fundamental plane of BH activity from AGNs to include blazars and GRBs. We utilize more accurate measurements of mass (Arabsalmani et al. 2018) to obtain a reliable fundamental plane. Our analysis reveals a fundamental plane that closely resembles the results obtained by Maccarone et al. (2003) and Merloni et al. (2003). The sample used in our study is presented in Section 2, and the correlation analysis results are discussed in Section 3. Finally, we present our conclusions in Section 4.

2. Sample

It is essential to have a sample of sources that have recorded X-ray luminosity (L_X), radio luminosity (L_R) and BH mass for the study of the fundamental plane. We compiled a sample of 50 radio-selected GRBs that have been observed in both the radio and X-ray wavelengths. These observations were obtained using radio telescopes between January 1997 and 2011 January (Chandra & Frail 2012; Lü et al. 2015).

$$L_R = 4\pi d_L^2 \nu F_R (1 + z)^{-\alpha_1 - 1}, \quad (1)$$

where d_L is the luminosity distance calculated from redshift z, and $d_L = z/H$ where $H = 73.4$ is the Hubble constant. F_R is the radio flux densities which are converted to the flux at 5 GHz by spectral slope $\alpha_1 = 1/3$ (Wang & Dai 2017). The X-ray luminosity of GRBs in 2–10 keV is measured with the X-ray flux densities in 0.3–10 keV which are converted to 2–10 keV from Chandra & Frail (2012) by using a power-law model with photon index $\tau = 0$ for long GRBs from the pre-Swift and post-Swift eras. GRBs have very powerful relativistic jets. For this reason, we should consider the influence of the beaming effect (Zhang et al. 2017). The intrinsic luminosities in X-ray and radio are measured by beaming factor f_b, $f_b \equiv 1 - \cos\theta$ where θ is the jet opening angle (Nemmen et al. 2012; Zhang et al. 2017).

$$f_b = 1 - \cos\theta_j. \quad (2)$$

θ_j is the jet opening angle of GRBs. We collected 43 GRB sources by cross matching other samples (Nemmen et al. 2012; Wang et al. 2014). With beaming factor f_b we can get the intrinsic luminosity in X-ray and radio.

$$\begin{aligned} L_{X^*} &= L_X f_b \\ L_{R^*} &= L_R f_b. \end{aligned} \quad (3)$$

L_{X^*} and L_{R^*} are the intrinsic luminosities in X-ray and radio, respectively. Because the central engine of most GRBs is still

unknown, it is difficult to measure the mass of GRBs. We only get 11 eligible GRBs with measured mass by cross matching with previous works. All the mass measurements of GRBs in this paper are taken from Arabsalmani et al. (2015, 2018). The mass of a GRB is estimated using a prescription based on empirical spectral energy distribution (SED) fitting, which has been summarized by previous researchers. Møller et al. (2013) proposed a method for calculating the stellar mass of quasi-stellar object-damped Lyman-α (QSO-DLA) galaxies based on their metallicity and redshift. Christensen et al. (2014) further improved this method by incorporating the influence of metallicity gradient. The stellar mass (M) can be calculated using the following equation

$$\log(M/M_\odot) = 1.76([M/H] + 0.022b + 0.35z + 5.04), \quad (4)$$

where [M/H] represents the measured metallicity of the DLA absorption, z denotes the redshift and b is the distance from the galaxy center (Møller et al. 2013). Arabsalmani et al. (2018) concluded that the stellar masses of GRB-DLA galaxies follow the same prescription as QSO-DLA galaxies and exhibit similar metallicity gradients to QSO-DLAs. They found that this formula remains valid for galaxies with stellar masses as low as $\log(M/M_\odot) = 8$. Using the formula proposed by Christensen et al. (2014), they calculated the predicted stellar masses of host galaxies in their sample. The measured masses were found to be in complete agreement with the results obtained through the procedure described by Glazebrook et al. (2004) and using the initial mass function given by Baldry & Glazebrok (2003). These findings demonstrate the reliability of this estimation method. In this study, we assume that the central structure of GRBs is a BH for the analysis of the fundamental plane relationship. The BH mass (M_{BH}) of a GRB can be estimated using the empirical formula proposed by Zachary et al. (2019), which relates the BH mass to the mass of the host galaxy

$$\begin{aligned} \log(M_{BH}/M_\odot) &= (1.24 \pm 0.08)\log(M/10^{11}M_\odot) \\ &+ (8.80 \pm 0.09), \end{aligned} \quad (5)$$

where M represents the mass of the host galaxy. The sample of GRBs with redshift (z), jet opening angle (θ_j), mass (M), BH mass (M_{BH}), X-ray luminosity (L_X) and radio luminosity (L_R) is listed in Table 1.

As is known, various types of AGNs have been observed to follow the fundamental plane (Körding et al. 2006; Li et al. 2008; Yuan et al. 2009; Gültekin et al. 2014). In our study, in order to compare with the GRBs, we not only utilized the sample of AGNs and BCGs from previous papers but also expanded our sample to include blazars. Blazars share many similarities with GRBs, such as the presence of relativistic jets and similar radiation processes (e.g., Gehrels et al. 2009; Lyu et al. 2014; Kumar & Zhang 2015; Wu et al. 2016; Mezcua et al. 2018). We collected 99 AGNs which are individual supermassive BH (SMBH) systems including 32 Seyfert 2 galaxies, 14 quasars, 19 Seyfert galaxies of type 1, 7 narrow

Table 1
The Masses of 05041, 050730, 050922C and 060206 are from Arabsalmani et al. (2015) by Predicting Which may have Error (⩽0.6) with Another Measured Mass of the Sample

[1] GRB	[2] z	[3] $\log L_R$	[4] $\log L_X$	[5] θ_j	[6] $\log M$	[7] $\log M_{BH}$
970508	0.835	41.44	45.28	21.6		
970828	0.958	40.76	45.97	7.1		
980425	0.009	38.78	40.69	11		
980703	0.966	41.75	45.83	11.2		
981226	1.11	40.9	45.28			
990510	1.619	41.58	46.78	3.4		
991216	1.02	41.96	46.64	4.6		
10222	1.477	41.04	46.99	3.2		
11211	2.14	41.68	47.8	6.4		
21004	2.33	43.2	46.56	12.7		
30226	1.986	42.33	46.59	3.43		
30329	0.169	42.3	45.63	5.1		
31203	0.105	39.48	43.08	9		
50401	2.898	41.88	47.41	5	8.8	6.07
050416A	0.65	40.76	45.66	5	9.23	6.61
050525A	0.606	40.32	45.89	5		
50603	2.821	42.34	47.36	5		
50730	3.968	42.45	48.08	5	6.73	3.51
050820A	2.615	41.86	48.1	6.6	8.96	6.27
50824	0.83	40.63	45.66	5	8.23	5.37
50904	6.29	42.48	46.37	8		
050922C	2.199	37.73	47.04	5	7.11	3.98
051016B	0.936	36.81	47.03	5	9.45	6.88
51022	0.809	40.85	47.12	5	9.84	7.36
60206	4.048	39.13	47.04		9.08	6.42
60218	0.033	38.15	43.08			
60418	1.49	41.42	46.13	5		
70125	1.548	42.8	46.77	13.2		
71003	1.604	41.95	46.98	5		
071010B	0.947	41.12	46.32	5		
71020	2.146	41.62	46.75	5		
080603A	1.687	41.53	46.49	5		
90313	3.375	42.59	47.53	3.08		
90323	3.57	42.4	47.53	2.8	10.29	7.92
90328	0.736	41.15	46.18	4.2		
90423	8.26	42.57	47.64	9.64		
90424	0.544	40.37	44.43	9.8		
090715B	3	42.11	46.82	1.39		
090902B	1.883	41.26	47.08	3.9		
91020	1.71	41.83	46.59	6.9		
100414A	1.368	41.71	47.22	5		
100418A	0.62	41.22	45.24	5	9.169	6.53
100814A	1.44	41.8	47.03	5		
100901A	1.408	42.2	47.05	5.72		
100906A	1.727	41.57	46.75	2.88		
111215A	2.06	42.55	47.65			
120326A	1.798	42.42	47.33			
130427A	0.34	41.4	46.92	5	8.92	6.22
130603B	0.3565	39.53	44.56			
130907A	1.238	42.15	47.44			

line Seyfert 1 galaxies (NS1), 11 low-ionization nuclear emission line regions (LINERS), 13 LINERS of type 2 and 2 LINER/H_{II} transition nuclei from Merloni et al. (2003). Most quoted values of this 2–10 keV X-ray and 5 GHz radio

luminosity taken from the literature are corrected with assumed $H_0 = 75$ km s^{-1} Mpc^{-1} when necessary. It should be noted that different methods used to measure BH mass vary in their effectiveness across all mass ranges (De Zeeuw 2003). In our study, we attempted to use sources with BH masses measured by the same method to ensure consistency. However, this may introduce a selection bias in the AGN data. The method used to measure BH masses in our AGN sample is the same as that used by Tremaine (2002). We aimed to gather a larger sample of eligible AGNs to ensure the reliability of the fundamental plane. Nevertheless, not all AGNs are easily observable in X-rays. For this reason, we extended our sample of AGNs by utilizing the correlation between X-ray luminosity and [O$_{III}$] $\lambda 5007$ optical emission-line luminosity, as derived by Heckman et al. (2005). This allowed us to include 21 type 1 sources in our AGN sample, with the X-ray luminosity in the 2–10 keV band estimated from the [O$_{III}$] luminosity. Additionally, BCGs have been confirmed to follow the fundamental plane (Mezcua et al. 2018).

We collected data for 72 BCGs, including determined BH mass, X-ray luminosity and radio luminosity, from Hogan et al. (2015), who conducted a multi-frequency radio study of BCGs drawn from a parent sample of 720 clusters selected in X-rays (Mezcua et al. 2018). For sources with available very long baseline interferometry (VLBI) radio observations, we directly measured the 5 GHz core radio flux (Mezcua et al. 2018), and for BCGs, we decomposed the radio emission into a core component using the radio SED. The X-ray emission of BCGs was calculated by subtracting the background counts scaled to the same number of pixels as the source region (Mezcua et al. 2018). We obtained the X-ray luminosity in the 2–10 keV band using the photometric method. The BH mass of BCGs was estimated using the K-band bulge luminosity with a correlation derived from Graham & Scott (2013).

Due to scarcity of observations, it is challenging to determine the Lorentz factor for all types of AGNs (types 1 and 2, Seyfert 1 and 2) and BCGs. Additionally, the X-ray and radio fluxes for some AGN sources may originate from the disk or corona. In this paper, we assume that the sample of AGNs and BCGs is isotropic.

Blazars share many similarities with GRBs, so establishing a unified fundamental plane relationship between blazars and GRBs will enhance our understanding of these sources. In this study, we compiled a sample of 87 blazars, comprising 27 BL Lacertae (BL Lac) objects, 50 flat spectrum radio quasars (FSRQs) and 10 uncertain blazars. To conduct the fundamental plane analysis, we considered their X-ray luminosity in the 2–10 keV range, 5 GHz radio luminosity and measured BH mass (Nemmen et al. 2012; Xiong et al. 2015). The 5 GHz radio luminosity and most X-ray luminosity data in the 2–10 keV range were obtained from the NASA/IPAC Extragalactic Database (NED). However, 16 blazars in our sample were missing X-ray flux density information in the

2–10 keV range. For these sources, we converted the X-ray flux densities provided by NED in the 0.2–10 keV or 0.3–10 keV range to the 2–10 keV range using a power-law model, employing a photon index τ of 2.47 for BL Lacs and 1.87 for FSRQs.

$$
\begin{aligned}
F_{2-10\text{keV}} &= F_{0.2-10\text{keV}} \frac{\int_{2\text{keV}}^{10\text{keV}} \nu^{1-\tau} d\nu}{\int_{0.2\text{keV}}^{10\text{keV}} \nu^{1-\tau} d\nu} \\
&= F_{2-10\text{keV}} \times 0.473581312 \\
F_{2-10\text{keV}} &= F_{0.3-10\text{keV}} \frac{\int_{2\text{keV}}^{10\text{keV}} \nu^{1-\tau} d\nu}{\int_{0.3\text{keV}}^{10\text{keV}} \nu^{1-\tau} d\nu} \\
&= F_{2-10\text{keV}} \times 0.473581312,
\end{aligned} \tag{6}
$$

where $F_{2-10\text{keV}}$, $F_{0.2-10\text{keV}}$ and $F_{0.3-10\text{keV}}$ respectively are the X-ray flux density in 2–10 keV, 0.2–10 keV and 0.3–10 keV. ν is the energy dissipation of blazars. Just like GRBs, blazars have very strong relativistic jets. Both X-ray and radio luminosity of blazars also should be considered with the influence of the beaming effect. We try to reduce the uncertainty between the data of blazars and GRBs. Thus, we also used f_b to measure the intrinsic luminosity of X-ray and radio luminosity (Nemmen et al. 2012; Zhang et al. 2017).

$$
f_b = 1 - \cos 1/\Gamma, \tag{7}
$$

where Γ denotes the bulk Lorentz factor of blazars. We identified 51 blazars with known values of the bulk Lorentz factor through cross-referencing previous literature (Nemmen et al. 2012; Xiong et al. 2015). The measured BH mass of the blazars was obtained directly from Cavagnolo et al. (2010). In our study, we compiled a total of 83 measured BH masses by cross-matching with Xiong et al. (2015). All details pertaining to our blazar sample, including redshift, type, X-ray luminosity, radio luminosity, beaming factor, measured BH mass (M_{BH}) and the corresponding measurement method (Reference), are presented in Tables 2 and 3.

In order to investigate the general properties of accretion, it is imperative to have a homogeneous sample of BHs that covers the entire range of BH masses (Saikia et al. 2015). To ensure the suitability of sources for our fundamental plane studies, we focused on XRBs due to the presence of various states in these systems (Remillard & McClintock 2006; Zhang et al. 2017). Our data set consists of 102 XRB sources specifically in the low/hard state, for which we obtained measurements of BH mass, X-ray luminosity and radio luminosity from Gallo et al. (2003) and Körding et al. (2006). The selected sources include GX 339-4 (Corbel et al. 2004), V404 Cyg (Corbel et al. 2004), XTE J1118+480 (Merloni et al. 2003) and A0620-00 (Gallo et al. 2003). Unlike blazars and GRBs, XRBs typically lack powerful relativistic

jets. Moreover, the majority of XRBs have wide jet opening angles ($\geqslant 60°$), rendering the effects of beaming negligible. Conversely, in the case of XRBs, the X-ray luminosity may not exhibit beaming effects if the origin of X-ray emission is from the disk or corona of the system. Thus, we assume that our XRB sample is isotropic, similar to AGNs and BCGs examined in our study.

3. Results

In this paper, we investigate the relationship between X-ray luminosity (L_X) and radio luminosity (L_R) for blazars and GRBs as part of our fundamental plane study. Similar to previous research, we find that this correlation exists not only in XRBs, AGNs and BCGs but can also be extended to blazars and GRBs. The left panel of Figure 1 illustrates this relationship between L_X and L_R for our entire sample. However, for GRBs, the correlation ($\log L_X = (0.88 \pm 0.01)\log L_R + 9.73 \pm 0.30$) is notably different from that of the entire sample. This discrepancy can be attributed to the strong influence of the beaming factor on both the X-ray and radio luminosities of blazars and GRBs, owing to their powerful relativistic jets. After accounting for the effect of beaming, we find that the correlation between L_X and L_R still persists for GRBs, blazars and AGNs, as shown in the right panel of Figure 1. Notably, the correlation for blazars ($\log L_X = (0.61 \pm 0.01)\log L_R + 17.92 \pm 0.28$) appears to be more similar to that of the entire sample ($\log L_X = (0.63 \pm 0.01)\log L_R + 17.38 \pm 0.47$) depicted in Figure 1. The fitting results for Figure 1 are in the Table 4. This suggests that the differences observed between blazars and AGNs may be attributed to the influence of the beaming effect. However, the correlation for GRBs remains distinct from that of the entire sample. This discrepancy can potentially be ascribed to the selection effect resulting from the limited number of available GRB data.

The influence of mass is very important for the correlation between the radio luminosity and X-ray luminosity. In this paper, we study the fundamental plane of our sample with measured mass. Our data are fitted by the function for the study of the fundamental plane in this paper.

$$
\log L_R = a \log L_X + b \log M + c, \tag{8}
$$

where L_R is the radio luminosity at 5 GHz, L_X is the X-ray luminosity in 2–10 keV, M is the mass of XRBs, AGNs and GRBs, and a, b and c are fitting parameters. By applying multivariate linear regression, we estimate the best-fit coefficients for this regression. The left panel of Figure 2 illustrates the fundamental plane for the entire sample, spanning approximately 18 orders of magnitude. The results of our best-fit regression model are $\log L_R = (0.81 \pm 0.02)\log L_X + (0.67 \pm 0.02)\log M - 1.22 \pm 0.79$. Notably, our findings differ significantly from previous work conducted by Gallo et al. (2003). Moreover, our analysis contrasts with the results

Table 2
The details of Blazar samples (I)

[1] Blazar	[2] z	[3] type	[4] $\log L_R$	[5] $\log L_X$	[6] f_b	[7] $\log M_{BH}$	[8] Reference
0106+013/4C+01.02	2.099	FSRQ	46.63	45.23	3.21	8.83	(6)
0133+476/OC 457	0.859	FSRQ	45.97	44.46	2.62	8.73	(1)
PMN J0157-4614	2.287	FSRQ	45.6	44.22		7.98	(1)
0219+428	0.444	BLL	45.23	43.53	2.64	8	(1)
0234+285/4C +28.07	1.213	FSRQ	46.3	44.64	2.52	9.22	(2)
0235+164/PKS 0235+164	0.94	BLL	46.21	44	2.66	9	(3)
B2 0242+23	2.247		46.47	44.15		9.12	(2)
0317+185	0.19	BLL	44.86	40.94		8.1	(4)
TXS 0322+222	2.066		47.02	44.64		9.5	(2)
0420-014/PKS 0420-01	0.916	FSRQ	45.84	44.66	2.4	9.03	(1)
PKS0426-380	1.111	BLL	45.68	44.4	3	8.6	(3)
0451-282/PKS 0451-28	2.56	FSRQ	46.99	45.3			
0454-234/PKS 0454-234	1.003	FSRQ	45.63	44.7			
0458-020/PKS 0458-020	2.291	FSRQ	46.44	45.28	2.74	9.27	(5)
0528+134	2.06	FSRQ	46.97	45.03		10.2	(6)
0537-441/PKS 0537-441	0.892	BLL	46.48	44.58		8.8	(3)
0537-286/PKS 0537-286	3.104	FSRQ	47.63	45.1			
0637-752/PKS 0637-75	0.653	FSRQ	45.78	44.4	2.49	9.41	(1)
B3 0650+453	0.928		45.09	43.37	2.65	8.17	(2)
0716+714	0.3	BLL	45.13	43.15	2.32	8.1	(6)
0735+178	0.424	BLL	44.7	43.14		8.4	(6)
0736+017/PKS 0736+01	0.189	FSRQ	44.57	42.86		8	(1)
B2 0743+25	2.979	FSRQ	47.71	44.71		9.59	(3)
TXS 0800+618	3.033		47.4	44.89		9.07	(2)
1ES 0806+524	0.138	BLL	45.68	41.36	1.89	8.9	(7)
OJ 535	1.418	FSRQ	46.22	44.37		9.42	(8)
B2 0827+24	0.94	FSRQ	45.71	44.09	3.1	9.01	(3)
0836+710/4C+71.07	2.172	FSRQ	48.16	44.95	3.2	9.36	(9)
0851+202/OJ 287	0.306	BLL	44.8	43.42	2.23	8.8	(3)
TXS 0907+230	2.661	FSRQ	45.82	43.92		8.7	(2)
B3 0908+41	2.563	FSRQ	45.85	43.97		9.32	(2)
B3 0917+449	2.19	FSRQ	46.98	44.74	3.12	9.25	(3)
4C+55.17	0.896	FSRQ	45.88	43.76	2.77	8.96	(3)
1ES 1011+496	0.212	BLL	45.96	42.01		8.3	(7)
B3 1030+415	1.117	FSRQ	45.64	44.3	2.59	8.65	(3)
PKS1057-79	0.581	BLL	44.92	43.99		8.8	(3)
1055+018/PKS 1055+01	0.888	BLL	45.85	44.61	2.19	8.45	(5)
Mkn 421	0.03	BLL	45.73	40.4	1.8	8.5	(3)
CRATES J1117+2014	0.139	BLL	44.5	40.9		8.62	(3)
1144-379/PKS 1144-379	1.048	FSRQ	45.43	44.16	2.58	8.5	(3)
PKS B1149-084	2.367	FSRQ	46.03	44.54		9.38	(2)
4C+29.45	0.724	FSRQ	45.61	43.91	3.1	9.18	(3)
1202-262/PKS 1203-26	0.789	FSRQ	45.63	43.94	2.46	8.59	(9)
1215+303	0.13	BLL	43.69	41.69	1.91	8.12	(10)
1ES 1218+304	0.184	BLL	45.4	41.34		8.6	(7)

References. The References of BH mass cited in the table are: (1) Woo & Urry (2002); (2) Michael et al. (2012); (3) Sbarrato et al. (2012); (4) Xie et al. (2004); (5) Zhou et al. (2009); (6) Chai et al. (2012); (7) Zhang et al. (2004); (8), Woo et al. (2005); (9), Liu et al. (2006); (10), Cao & Jiang (1999).

presented by Plotkin et al. (2012), who observed that relativistically beamed BL Lac sources align well with the fundamental plane. However, the outcomes obtained from our sample, comprising 27 BL Lacs and 50 FSRQs, deviate from those reported by Plotkin et al. (2012). The left panel of Figure 2 shows the fundamental plane for BH activity with GRBs. The fitting results for Figure 2 are in Table 5.

Blazars and GRBs are known to exhibit strong relativistic jets. In our study, we find that the X-ray and radio luminosity of blazars and GRBs is highly beamed. To account for this beaming effect, we estimate the intrinsic luminosity of the X-ray and radio emissions by applying the beaming factor, f_b (Nemmen et al. 2012). The right panel of Figure 2 presents the fundamental plane of the entire sample, incorporating the

Table 3
The details of Blazar samples (II)

[1] Blazar	[2] z	[3] type	[4] $\log L_R$	[5] $\log L_X$	[6] f_b	[7] $\log M_{BH}$	[8] Reference
1219+285	0.102	BLL	43.38	41.56	1.91	7.4	(6)
4C+21.35	0.432	FSRQ	45.29	43.23	3.61	8.87	(3)
1226+023/3C 273	0.158	FSRQ	46.1	44.09	2.58	8.9	(3)
1244-255	0.633	FSRQ	45.23	43.79	2.64	9.04	(10)
1253-055/3C 279	0.536	FSRQ	46.14	44.66	2.94	8.9	(3)
1308+326/B2 1308+32	0.996	FSRQ	45.97	44.18	2.99	8.8	(3)
PMN J1344-1723	2.506	FSRQ	45.66	44.44		9.12	(2)
B3 1343+451	2.534	FSRQ	46.1	44.36		8.98	(2)
1406+076	1.494	FSRQ	45.97	44.43		9.4	(6)
1424-418/PKS 1424-41	1.522	FSRQ	46.52	44.94	3.02		
1426+428	0.129	BLL	45.11	40.59		9.13	(10)
PKS 1502+106	1.839	FSRQ	46.58	44.61	2.66	9.64	(3)
1508-055	1.185	FSRQ	45.6	44.61	2.72	8.97	(6)
1510-089/PKS 1510-08	0.361	FSRQ	45.29	43.71	2.93	8.6	(3)
1514-241	0.049	BLL	43	41.91	1.67	8.1	(10)
B2 1520+31	1.484	FSRQ	45.6	44.09		8.92	(2)
MG2 J153938+2744	2.191	FSRQ	45.84	43.89		8.43	(2)
4C+05.64	1.422	FSRQ	46.33	44.91	2.64	9.38	(3)
1633+382/4C+38.41	1.814	FSRQ	46.6	45.09	3.29	9.53	(3)
Mkn 501	0.034	BLL	44.08	41.24	1.66	9	(3)
I Zw 187	0.055	BLL	43.81	40.64	1.44	7.86	(10)
4C+09.57/PKS1749+096	0.322	BLL	45.12	43.45	2.1	8.7	(3)
CGRaBS J1800+7828/S5 1803+78	0.68	BLL	45.56	44.13	2.25	8.6	(3)
3C 371	0.051	BLL	43.29	41.52	0.34	8.7	(3)
B2 1846+32	0.798		45.13	43.41		7.87	(2)
1849+670/CGRaBS J1849+6705	0.657	FSRQ	45.47	43.85	2.61	9.14	(1)
PMN J1959-4246	2.178	FSRQ	46.14	44.1		8.55	(2)
1ES 1959+650	0.047	BLL	44.68	40.7		8.1	(7)
PKS 2005-489	0.071	BLL	44.36	41.75		8.5	(3)
OX 131	2.18	FSRQ	45.57	44.29		7.75	(2)
OX 169	0.211	FSRQ	44.28	42.57	2.19	8.6	(3)
2145+067/4C+06.69	0.99	FSRQ	46.88	44.89	2.1	8.87	(9)
B2 2155+31	1.488		46.05	44.11		8.89	(2)
PKS 2155-304	0.116	BLL	44.91	41.74	2.65	8.7	(7)
BL Lac	0.069	BLL	44	42.05	1.77	8.7	(3)
PKS 2209+236	1.125		45.46	44.15		8.46	(2)
PKS 2227-08	1.56	FSRQ	46.63	44.85	2.3	8.95	(3)
2230+114/CTA 102	1.037	FSRQ	46.38	44.94	2.68	8.7	(3)
2251+158/3C 454.3	0.859	FSRQ	46.8	45.01	2.78	8.7	(3)
2255-282/PKS 2255-282	0.926	FSRQ	45.79	44.43	2.65	8.92	(9)
PKS 2325+093	1.841		46.84	44.29		8.7	(2)
PMN J2345-1555	0.621		44.58	43.46		8.16	(2)

References. The References of BH mass cited in the table are: (1) Woo & Urry (2002); (2) Michael et al. (2012); (3) Sbarrato et al. (2012); (4) Xie et al. (2004); (5) Zhou et al. (2009); (6) Chai et al. (2012); (7) Zhang et al. (2004); (8) Xiong et al. (2015); (9) Liu et al. (2006); (10) Mohaupt (2003).

intrinsic luminosity of X-ray and radio emissions. Using multivariate regression analysis, we obtain the following result for the entire sample: $\log L_R = (0.60 \pm 0.03)\log L_X + (0.78 \pm 0.02)\log M + 7.22 \pm 0.95$, which is in good agreement with Equation (1) of Maccarone et al. (2003). The r value is 0.97. The highest correlation was obtained by analyzing the whole sample compared to the classified sample. The significance of each variable is 0.005, less than 0.05. It shows that the fitting results are reliable and the fundamental relation is valid. Due to

the limited availability of data on eligible GRBs with measured mass, we combined the sample of GRBs and blazars to analyze the fundamental plane, thus minimizing the effects of selection bias. This approach also facilitated the examination of the uniformity observed between GRBs and AGNs, considering the numerous similarities between blazars and GRBs outlined in this study. Furthermore, our study reveals that the fundamental plane for blazars and GRBs, $\log L_R = (0.55 \pm 0.12) \log L_X + (1.02 \pm 0.11) \log M + 9.531 \pm 5.50$, remains
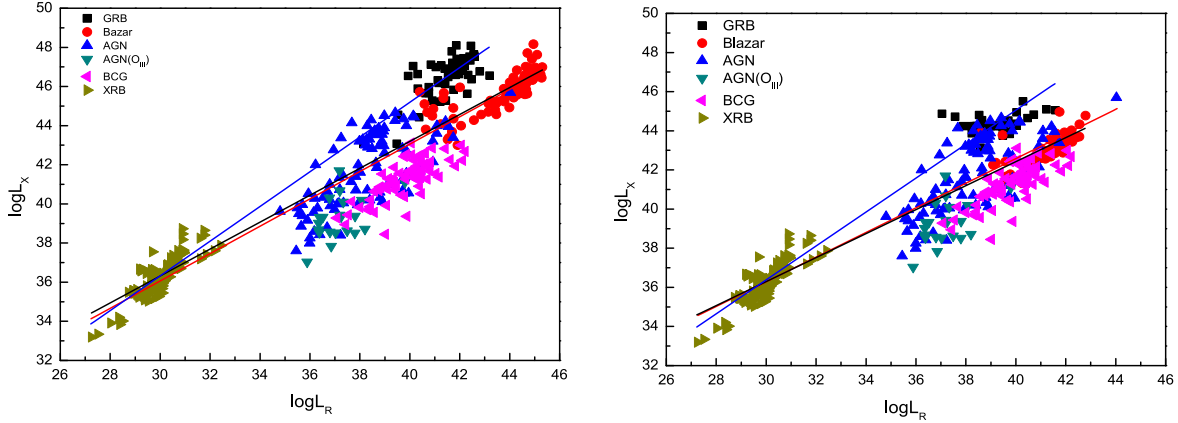
Figure 1. Left panel: The correlation between L_X and L_R. The red line is the best fitting for the whole sample. The blue line represents the best fitting of GRBs. The black line is the best fitting for the blazars. Right panel: The correlation between L_X and L_R with beaming corrected. The red line is the best fitting for the whole sample. The blue line represents the best fitting of GRBs. The black line is the best fitting for the blazars.

Table 4
The Results of Correlation Analysis for the Sample in Figure 1

Parameter	r	p
GRB	0.88	0.002
Blazar	0.84	0.001
Whole sample	0.98	0.003
GRB[a]	0.96	0.005
Blazars[a]	0.96	0.002
Whole sample with GRB[a] and Blazars[a]	0.97	0.005

Note. The r is correlation coefficient; p is significance level;
[a] Indicates that the corresponding data have been corrected with beaming factor.

consistent with the results obtained for the entire sample, even after accounting for the beaming effect ($\log L_R = (0.48 \pm 0.19) \log L_X + (0.61 \pm 0.12) \log M + 14.81 \pm 8.66$). This suggests that blazars and GRBs align well with the fundamental plane. Notably, when considering the beaming effect, the slope of the fundamental plane experiences a substantial change. Specifically, for parameter a, the slope changes from 0.81 ± 0.02 to 0.52 ± 0.07, and for parameter b, it changes from 0.67 ± 0.02 to 0.51 ± 0.08. These observations indicate a strong dependence of the fundamental plane on the beaming factor, which competes with previous studies conducted by Körding et al. (2006) and Wang & Dai (2017). Additionally, after accounting for the beaming effect, the data points of GRBs and blazars exhibit closer proximity to AGNs. This suggests that certain disparities previously attributed to differences between blazars and AGNs could be attributed to the beaming effect, thus implying that some GRBs may share similar characteristics with AGNs (Lyu et al. 2014; Wu et al. 2016).

4. Summary

This paper validates previous findings regarding the existence of a fundamental plane of BH activity. The fundamental plane refers to the correlation between the radio luminosity, X-ray luminosity and BH mass among different types of BHs, including stellar-mass, intermediate-mass and supermassive BHs. The study confirms that this fundamental plane, initially observed in XRBs in the low/hard state and AGNs, can also be extended to blazars and GRBs. By considering the beaming factor, the results ($\log L_R = (0.60 \pm 0.03) \log L_X + (0.78 \pm 0.02) \log M + 7.22 \pm 0.95$) are consistent with previous studies conducted by Merloni et al. (2003) and Maccarone et al. (2003). Notably, some data points of blazars even coincide with AGNs (please see the right panel of Figure 2), suggesting that the variations observed between blazars and normal AGNs (type 1 and type 2) may be attributed to the beaming effect. This finding also holds significant implications for the understanding of GRBs. The similarity between GRBs and AGNs could potentially be explained by their central engines being BHs. This sheds light on the physics of GRBs and can help measure the mass of GRBs with unknown mass using the derived fundamental plane. Additionally, the study observes that the slope of the fundamental plane changes substantially when the beaming effect is considered. This suggests that the fundamental plane is partly dependent on the beaming factor, contrary to the conclusion of Wang & Dai (2017), which expanded the sample of the fundamental plane by assuming BH masses for GRBs. The difference in findings may be attributed to the small sample size of GRBs with measured masses in this study, as well as the inclusion of blazars with strong relativistic jets. Consequently, the beaming effect should be taken into account when considering the fundamental plane of blazars and GRBs.
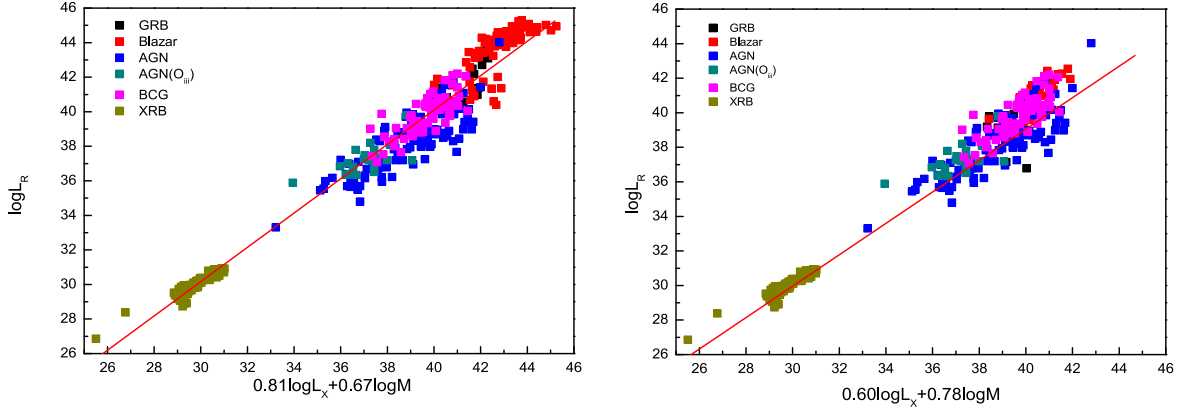
Figure 2. Left panel: The fundamental plane of BH activity with GRBs. The red line is the best fitting for all samples ($\log L_R = (0.81 \pm 0.02)\log L_X + (0.67 \pm 0.02)$ $\log M - 1.22 \pm 0.79$. Right panel: The fundamental plane of BH activity with beaming corrected. The red line is the best fitting for all samples which include the beaming corrected data of blazars ($\log L_R = (0.60 \pm 0.03)\log L_X + (0.78 \pm 0.02)\log M + 7.22 \pm 0.95$.

Table 5
The Results of Best Fitting Analysis for the Sample in Figure 2

Parameter	r	$p(L_X)$	$p(M)$
GRB and Blazar	0.72	0.001	0.001
Whole sample	0.96	0.001	0.001
GRB[a] and Blazars[a]	0.54	0.001	0.012
Whole sample with GRB[a] and Blazars[a]	0.93	0.001	0.001

Note. The r is correlation coefficient; $p(L_X)$ is significance level of $\log L_X$; $p(M)$ is significance level of $\log M$;
[a] Indicates that the corresponding data have been corrected with beaming factor.

In this paper, we are unable to draw a definitive conclusion regarding the two competing explanations for the fundamental plane. While most of our sample can be considered as sources that align with jet-dominated models, such as XRBs and AGNs, the inclusion of 50 FSRQs (a type of blazar) in our study also demonstrates a good fit with the fundamental plane. However, it is worth noting that the X-ray luminosity of some FSRQs is believed to originate from both the accretion disk and the jet. Further investigation with a larger sample size is needed to explore this in more detail. We have also observed that the correlation between the X-ray luminosity and radio luminosity of GRBs differs significantly from the overall sample. This discrepancy may be due to the small number of GRBs with available information on jet opening angle and measured mass, which introduces selection effects, or it could be a result of observation errors in our study. To address this, we have combined the sample of blazars and GRBs as a whole, as they share similar characteristics (Lyu et al. 2014; Wu et al. 2016), to measure the fundamental plane and minimize the impact of selection effects. Nonetheless, this combination introduces additional uncertainty to our results. In order to evaluate the reliability of the fundamental plane, it is generally considered

ideal to have quasi-simultaneous measurements of radio and X-ray luminosity. This is particularly important for GRBs and blazars due to the cooling mechanism of the GRB and the light variability of the blazars. These factors cause the radio and X-ray luminosity of these samples to vary over time, which in turn affects the analysis results of the fundamental plane. This variation leads to a decrease in the correlation of R-values and an increase in the significance of the results. However, obtaining simultaneous observations is rare, and most of the data for AGNs, BCGs, blazars and GRBs in our study are non-simultaneous measurements. Miller et al. (2010) suggested that individual sources may not strictly conform to the fundamental plane on short timescales (Wang & Dai 2017). Additionally, Wang & Dai (2017) found that the time lags observed in GRBs (Chandra & Frail 2012; Lü et al. 2015) and blazars (Angel & Stockman 1980; Urry & Padovani 1995; Xiong et al. 2015) in our study could be similar to those observed in AGNs.

ORCID iDs

Quan-Gui Gao ⓘ https://orcid.org/0000-0001-9732-069X

References

Angel, J. R. P., & Stockman, H. S. 1980, ARA&A, 18, 321
Arabsalmani, M., Møller, P., Freudling, W., et al. 2018, MNRAS, 473, 3312
Arabsalmani, M., Møller, P., Fynbo, J. P. U., et al. 2015, MNRAS, 446, 990
Baldry, I. K., & Glazebrok, K. 2003, ApJ, 593, 258

Chai, B., Cao, X., & Gu, M. 2012, ApJ, 759, 114
Cao, X., & Jiang, D. R. 1999, MNRAS, 307, 802
Cavagnolo, K. W., McNamara, B. R., Nulsen, P. E. J., et al. 2010, ApJ, 720, 1066
Chandra, P., & Frail, D. A. 2012, ApJ, 746, 156
Christensen, L., Møller, P., Fynbo, J. P. U., et al. 2014, MNRAS, 445, 225
Constantinos, K., Zorawar, W., Alice, K. H., et al. 2022, AJ, 934, 65
Corbel, S., Fender, R. P., Tomsick, J. A., et al. 2004, ApJ, 617, 1272
Corbel, S., Fender, R. P., Tzioumis, A. K., et al. 2000, A&A, 359, 251
Coriat, M., Corbel, S., Prat, L., et al. 2011, MNRAS, 414, 677
De Zeeuw, T. 2003, ASPC, 291, 205
Dong, A., Wu, Q. W., & Cao, X. F. 2014, ApJL, 787, L20
Eichler, D., Livio, M., Piran, T., et al. 1989, Natur, 340, 126
Falcke, H., Körding, E., & Markoff, S. 2004, A&A, 414, 895
Gallo, E., Fender, R. P., & Pooley, G. G. 2003, MNRAS, 344, 60
Gehrels, N., Ramirez-Ruiz, E., & Fox, D. B. 2009, ARA&A, 47, 567
Glazebrook, K., Abraham, R. G., McCarthy, P. J., et al. 2004, Natur, 430, 181
Graham, A. W., & Scott, N. 2013, ApJ, 764, 151
Gültekin, K., Cackett, E. M., King, A. L., Miller, J. M., & Pinkney, J. 2014, ApJL, 788, L22
Heckman, T. M., Ptak, A., Hornschemeier, A., & Kauffmann, G. K. 2005, AJ, 634, 161
Hogan, M. T., Edge, A. C., Geach, J. E., et al. 2015, MNRAS, 453, 1201
Jonker, P. G., Miller-Jones, J., & Homan, J. 2010, MNRAS, 401, 1255
Körding, E., Falcke, H., & Corbel, S. 2006, A&A, 456, 439
Kumar, P., & Zhang, B. 2015, PhR, 561, 1
Li, Z., Wu, X. B., & Wang, R. 2008, ApJ, 688, 826
Liu, Y., Jiang, D. R., & Gu, M. F. 2006, ApJ, 637, 669
Lü, J., Perkins, A., Pope, C. N., et al. 2015, RAA, 15, 617
Lyu, F., Liang, E.-W., Liang, Y.-F., et al. 2014, ApJ, 793, 36
Maccarone, T. J., Gallo, E., & Fender, R. 2003, MNRAS, 345, L19
McHardy, I. M., Köding, E., Knigge, C., et al. 2006, Natur, 444, 739
Meier, D. L. 2003, NewA, 47, 667
Merloni, A., Heinz, S., & Di Matteo, T. 2003, MNRAS, 345, 1057
Merloni, A., Köding, E., Heinz, S., Markoff, S., et al. 2006, NewA, 11, 56
Mezcua, M., Hlavacek-Larrondo, J., Lucey, J. R., et al. 2018, MNRAS, 474, 1342
Michael, S., Steiman-Cameron, T. Y., Durisen, R. H., & Boley, A. C. 2012, ApJ, 746, 98
Miller, J. M., Nowak, M., Marko, S., et al. 2010, ApJ, 720, 1033
Mirabel, I. F., & Rodriguez, L. F. 1999, ARA&A, 37, 409
Mohaupt, T. 2003, Introduction to String Theory, Quantum Gravity,Lecture Notes in Physics (Berlin: Springer), 173
Møller, P., Fynbo, J. P. U., Ledoux, C., & Nilsson, K. K. 2013, MNRAS, 430, 2680
Nakar, E. 2007, PhR, 442, 166
Nemmen, R. S., Georganopoulos, M., Guiriec, S., et al. 2012, Sci, 338, 1445
Piran, T. 2004, RvMP, 76, 1143
Plotkin, R. M., Markoff, S., Kelly, B. C., et al. 2012, MNRAS, 419, 267
Ratti, E. M., Jonker, P. G., Miller-Jones, J. A. C., et al. 2012, MNRAS, 423, 2656
Remillard, R. A., & McClintock, J. E. 2006, ARA&A, 44, 49
Saikia, P., Körding, E., & Falcke, H. 2015, MNRAS, 450, 2317
Sbarrato, T., Ghisellini, G., Maraschi, L., & Colpi, M. 2012, MNRAS, 421, 1764
Tremaine, S. 2002, ApJ, 574, 740
Urry, C. M., & Padovani, P. 1995, PASP, 107, 803
Wang, F. Y., & Dai, Z. G. 2017, MNRAS, 470, 1101
Wang, F. Y., Dai, Z. G., & Liang, E. W. 2015, NewAR, 67, 1
Wang, F. Y., Yi, S. X., & Dai, Z. G. 2014, ApJL, 786, L8
White, N. E., Fabian, A. C., & Mushotzky, R. F. 1984, A&A, 133, 9
Woo, J.-H., & Urry, C. M. 2002, ApJ, 579, 530
Woo, J.-H., Urry, C. M., van der Marel, R. P., Lira, P., & Maza, J. 2005, ApJ, 631, 762
Woosley, S. E. 1993, ApJ, 405, 273
Wu, Q., Metzger, B. D., Gabriel, et al. 2016, MNRAS, 455, L1
Xie, F., & Yuan, F. 2017, ApJ, 836, 1
Xie, G. Z., Zhou, S. B., & Liang, E. W. 2004, AJ, 127, 53
Xiong, D. R., Bai, J. M., Fan, J. H., et al. 2020, ApJS, 247, 49
Xiong, D. R., Bai, J. M., Zhang, H. J., et al. 2017, ApJS, 229, 21
Xiong, D. R., & Zhang, X. 2014, MNRAS, 441, 3375
Xiong, D. R., Zhang, X., Bai, J. M., & Zhang, H. J. 2015, MNRAS, 450, 3568
Yuan, F., Yu, Z., & Ho, L. C. 2009, ApJ, 703, 1034
Zachary, S., Amy, E. R., & Jenny, E. G. 2019, ApJ, 887, 245
Zhang, B., & Mészáros, P. 2004, IJMPA, 19, 2385
Zhang, X., Zhang, H. J., Zhang, X., et al. 2017, Ap&SS, 362, 244
Zhou, M., & Cao, X.-W. 2009, RAA, 9, 293
Zhu, B. T., Zhang, L., & Fang, J. 2019, ApJ, 873, 120